

# Pion and Kaon Vector Form Factors

J. A. Oller

*Forschungszentrum Jülich, Institut für Kernphysik (Theorie)  
D-52425 Jülich, Germany*

E. Oset and J. E. Palomar

*Departamento de Física Teórica e IFIC, Centro Mixto Universidad de Valencia-CSIC,  
46100 Burjassot (Valencia), Spain*

## Abstract

We develop a unitarity approach to consider the final state interaction corrections to the tree level graphs calculated from Chiral Perturbation Theory ( $\chi PT$ ) allowing the inclusion of explicit resonance fields. The method is discussed considering the coupled channel pion and kaon vector form factors. These form factors are then matched with the one loop  $\chi PT$  results. A very good description of experimental data is accomplished for the vector form factors up to  $\sqrt{s} \leq 1.2$  GeV beyond which multiparticle states play a non negligible role. For the P-wave  $\pi\pi$  phase shifts the agreement with data stands even higher up to  $\sqrt{s} \leq 1.5$  GeV. We also consider the isospin breaking effects due to the  $\omega - \rho$  mixing as a perturbation to the previous results. In addition the low and resonance energy regions are discussed in detail and for the former a comparison with one and two loop  $\chi PT$  is made showing a remarkable coincidence with the two loop  $\chi PT$  results.

## 1 Introduction

The study of the pion vector form factor is an interesting problem mainly because pions are the lightest hadrons and hence they are common products in many experiments so that a good description of the pion electromagnetic form factor is often required.

Many of the studies of this problem deal with some kind of modified vector meson dominance (VMD) [1] when taking into account the effects of unitarity and final state interactions. This was done long time ago in ref. [2] and it was found that these effects show up not only as a modification of the bare  $\rho$  propagator but also as a change in its bare couplings. Other more phenomenological parameterizations are the ones in refs. [3, 4], which basically account for the dressing of the bare  $\rho$  propagator and allow to add more resonances and parameters in order to fit the data up to high energies, hiding in this way extra effects as the presence of multiparticle channels, e.g.  $4\pi$ ,  $\omega\pi$  etc... This latter kind of expressions are the ones commonly used in many experimental papers in order to fit their data and determine the resonance content.

It is well known that the low energy effective theory of QCD is Chiral Perturbation Theory ( $\chi PT$ ) [5, 6, 7]. Although this is a systematic way to express the QCD Green functions in terms of a power momentum expansion, unfortunately, it is valid only for low energies. Hence, if one is interested in higher energies nonperturbative schemes are unavoidable. Nevertheless, one should demand that, when used at low energies, these nonperturbative methods reproduce the low energy constraints of QCD given by the  $\chi PT$  expansion.

The approach described in sections 2 and 3 reproduces the one loop  $\chi PT$  pion and kaon vector form factors [7] and, as we show below, it is also appropriate to study higher energies by satisfying unitarity in coupled channels and incorporating explicit resonance fields [8]. In this latter reference it is discussed how, at lowest order in the chiral expansion, resonances with spin  $\leq 1$  couple with pseudoscalars ( $\pi$ ,  $K$ ,  $\eta$ ) and with electroweak currents. It is also shown there how to connect with the standard VMD picture, when taking into account results from large  $N_c$  and QCD high energy constraints.

Other nonperturbative approaches that match with the one loop  $\chi PT$  vector pion form factor are given in refs. [9, 10, 11]. In ref. [12, 13] the matching is given up to the two loop  $SU(2) \times SU(2)$   $\chi PT$  pion vector form factor first calculated numerically in [13] and then analytically in [14]. While the work of ref. [13] is only interested in assessing the relevance of higher order loops at low energies, the works of refs. [9, 10, 11, 12] make predictions at higher energies, although all of them take into account only elastic unitarity. Ref. [9], as ref. [13], makes use of an Omnès representation<sup>1</sup> [15] but allowing for the explicit presence of the  $\rho$  resonance [8]. In ref. [11] the pion vector form factor is studied by solving the Bethe-Salpeter equation making some assumptions on the off shell extrapolation of the amplitudes and using only the  $\pi\pi$  channel. On the other hand, in ref. [10, 12] [0,1] and [0,2] Padé approximants from the  $\chi PT$  results are used (see also the discussions in refs. [13, 16] with respect the former references). Finally in refs. [17, 18] an Omnès parameterization, assuming elastic unitarity, is implemented using directly the experimental  $I=1$  P-wave  $\pi\pi$  phase shifts.

In our work the isospin limit is taken but we shall also estimate the effect of the isospin violating  $\omega - \rho$  mixing in the pion vector form factor. This contribution manifests itself in a very narrow energy range to the right of the peak of the  $\rho$  mass distribution in accordance with the mass and small width of the  $\omega$  (see fig.7). Other works in which this effect has been already discussed are [4, 19, 20]. On the other hand, when comparing our results for the vector pion form factor in the  $\rho$  region with the experimental data, we shall also take data from  $\tau$ -decays [21] in which only the  $I = 1$  part of the vector pion form factor contributes. Finally, in ref. [22] the isospin breaking effects in the pion form factors for the low energy regime are studied at next-to-leading order in  $SU(2) \times SU(2)$   $\chi PT$ .

## 2 Tree level

We will evaluate the tree level vector form factors and scattering amplitudes making use of the lowest order  $\chi PT$  Lagrangian [7] plus the chiral resonance Lagrangians [8]. These tree level amplitudes will be leading in large  $N_c$ , while non leading contributions in this counting will be generated through the unitarization process to be discussed in the next section.

In the case of the vector  $\pi\pi$  and  $K\bar{K}$  form factors we have to evaluate the diagrams

---

<sup>1</sup>Although in the end, since only the real part of the exponent of the exponential is kept, some of the analytical properties of the form factor are lost.

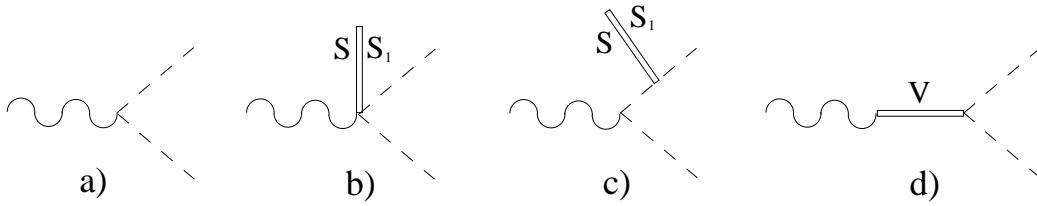


Figure 1: Diagrams considered for calculating the tree level form factors, eqs. (2). From left to right: a)  $\chi PT$  lowest order. b) Octet,  $S$ , and singlet,  $S_1$ , scalar resonance exchanges coupled to the vacuum. c) Wave function renormalization from the exchange of scalar resonances and d) exchange of vector resonances,  $\rho$ ,  $\omega$  and  $\phi$ . Fig. 1a is calculated from ref. [7] and the rest from ref. [8].

depicted in fig.1. The contributions from the diagram of fig.1b and the ones from the wave function renormalization, fig.1c, cancel each other due to charge conservation. A similar set of diagrams has been considered in ref. [24] in order to study the coupled  $K\pi$ ,  $K\eta$  and  $K\eta'$  scalar form factors [25]. In the former reference, although restricted to the study of the associated S-wave  $I=1/2$  meson-meson  $T$ -matrix, the requirement that the form factors vanish at  $s \rightarrow \infty$  is used to reduce the number of free parameters.

On the other hand, we will assume ideal mixing between the  $\omega_8$  and  $\omega_1$  resonances, so that the  $\omega$  and  $\phi$  are given by

$$\begin{aligned}\omega &= \frac{2}{\sqrt{6}}\omega_1 + \frac{1}{\sqrt{3}}\omega_8 \\ \phi &= \frac{1}{\sqrt{3}}\omega_1 - \frac{2}{\sqrt{6}}\omega_8\end{aligned}\tag{1}$$

and we will work explicitly in terms of the  $\omega$  and  $\phi$  mesons. In this way we will be able to distinguish between the different physical masses of the  $\omega$  and  $\phi$  resonances. Note that at the order considered in ref. [8] vector singlet resonances,  $\omega_1$ , do not couple neither to photons nor to pseudoscalars.

The resulting tree level vector form factors for the  $\pi^+\pi^-$ ,  $K^+K^-$  and  $K^0\bar{K}^0$  systems are:

$$\begin{aligned}F_{\pi\pi}^t(s) &= 1 + \frac{F_V G_V}{f^2} \frac{s}{M_\rho^2 - s} \\ F_{K^+K^-}^t(s) &= 1 + \frac{F_V G_V}{2f^2} s \left[ \frac{1}{M_\rho^2 - s} + \frac{1}{3} \frac{1}{M_\omega^2 - s} + \frac{2}{3} \frac{1}{M_\phi^2 - s} \right] \\ F_{K^0\bar{K}^0}^t(s) &= \frac{F_V G_V}{2f^2} s \left[ -\frac{1}{M_\rho^2 - s} + \frac{1}{3} \frac{1}{M_\omega^2 - s} + \frac{2}{3} \frac{1}{M_\phi^2 - s} \right]\end{aligned}\tag{2}$$

where  $F_V$  measures the strength of the photon-vector resonance vertex,  $G_V$  the same but for the pseudoscalar-vector resonance ones and  $s$  is the usual Mandelstam variable. Finally,  $M_\rho$ ,  $M_\omega$  and  $M_\phi$  refer to the bare masses of the  $\rho$ ,  $\omega$  and  $\phi$  resonances and  $f$  is the pion decay constant,  $f_\pi$ , in the chiral limit [7].

One can proceed analogously for the evaluation of the tree level scattering amplitudes between the former states. In ref. [26] similar tree level amplitudes were already calculated

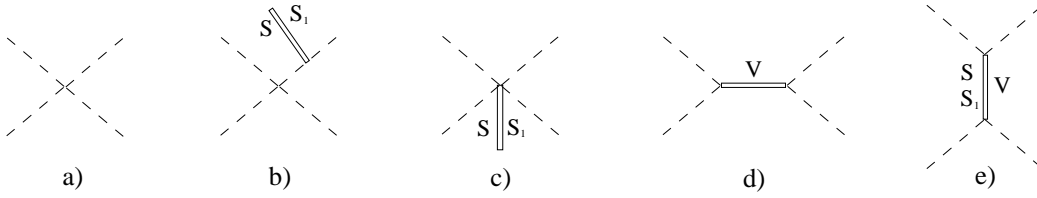


Figure 2: Diagrams considered for calculating the tree level amplitudes, eqs. (3). From left to right: a)  $\chi PT$  lowest order. b) Wave function renormalization from the exchange of scalar resonances. c) Tadpole-like diagram with the exchange of scalar resonances coupled to the vacuum. d) Exchange of vector resonances,  $\rho$ ,  $\omega$  and  $\phi$ , in the  $s$ -channel and e) crossed exchange of vector and scalar resonances. Fig. 2a is calculated from ref. [7] and the rest from ref. [8].

in the same way for studying the elastic  $\pi\pi$  and  $K\pi$  scattering. In addition, in ref. [24] the  $K\eta$  and  $K\eta'$  channels were also included to study the  $K\pi$  scattering up to 2 GeV. The corresponding generic set of diagrams is indicated in fig.2. However, out of these diagrams we are not going to consider explicitly here those corresponding to the exchange of resonances in the crossed channels, fig.2e. The reason is twofold: 1) they are not necessary to match with the one loop  $\chi PT$  results for the  $SU(3)$  vector form factors [7] since they give rise to higher orders. 2) Because of VMD one expects a good description of the scattering amplitudes in the physical region when including the  $s$ -channel exchange of the vector resonances together with unitarity. With respect to the second point one has to take into account that in the chiral Lagrangians [7, 8] the standard picture of VMD [23] is only accomplished when considering the lowest order  $\chi PT$  contribution together with the explicit resonance fields [27, 9]. Furthermore, when making a dispersive analysis of the vector form factors, only the scattering amplitudes in the physical region are involved (see next section).

The resulting P-wave <sup>2</sup> partial wave amplitudes are:

$$\begin{aligned}
T(s)_{\pi^+\pi^-, \pi^+\pi^-} &= \frac{2}{3} \frac{p_\pi^2}{f^2} \left[ 1 + \frac{2G_V^2}{f^2} \frac{s}{M_\rho^2 - s} \right] \\
T(s)_{\pi^+\pi^-, K^+K^-} &= \frac{p_\pi p_K}{3f^2} \left[ 1 + \frac{2G_V^2}{f^2} \frac{s}{M_\rho^2 - s} \right] \\
T(s)_{\pi^+\pi^-, K^0\bar{K}^0} &= -T(s)_{\pi^+\pi^-, K^+K^-} \\
T(s)_{K^+K^-, K^+K^-} &= \frac{2}{3} \frac{p_K^2}{f^2} \left[ 1 + \frac{G_V^2}{2f^2} \frac{s}{M_\rho^2 - s} + \frac{G_V^2}{2f^2} \frac{s}{M_\omega^2 - s} + \frac{G_V^2}{f^2} \frac{s}{M_\phi^2 - s} \right] \\
T(s)_{K^0\bar{K}^0, K^0\bar{K}^0} &= T_{K^+K^-, K^+K^-}(s) \\
T(s)_{K^+K^-, K^0\bar{K}^0} &= \frac{p_K^2}{3f^2} \left[ 1 + \frac{G_V^2}{f^2} \frac{s}{M_\omega^2 - s} + \frac{2G_V^2}{f^2} \frac{s}{M_\phi^2 - s} - \frac{G_V^2}{f^2} \frac{s}{M_\rho^2 - s} \right] \quad (3)
\end{aligned}$$

By writing the lowest order amplitudes in terms of  $f$ , there is a cancelation between the

---

<sup>2</sup>A partial wave amplitude with angular momentum  $L$  is defined to be  $\frac{1}{2} \int_{-1}^1 d\cos\theta P_L(\cos\theta) T(s, t, u)$  where  $P_L(\cos\theta)$  is the Legendre polynomial of  $L_{th}$  degree,  $T(s, t, u)$  is the scattering amplitude and  $s, t$  and  $u$  are the usual Mandelstam variables.

contributions of the wave function renormalization terms, fig. 2b, those of the exchange of the scalar resonances coupled to the vacuum, fig. 2c, and the  $\mathcal{O}(p^4)$  crossed channel scalar contributions absorbed in the  $\mathcal{O}(p^4)$   $\chi PT$  term proportional to the  $L_5$  counterterm [7, 8], fig. 2e. Consistently with our approach of working the large  $N_c$  leading contributions from ref. [7], we have taken the masses of the scalar singlet and octet equal and we have also made use of the relation between their couplings deduced in ref. [8]. In this way, for instance, one has that  $L_4 = L_6 = 0$  consistently with phenomenology [28] and with the fact that both are subleading counterterms in large  $N_c$ .

### 3 Unitarization

We will deduce our final expressions for the form factors after deriving those of the  $T$ -matrix. The latter will be accomplished by unitarizing the tree level scattering amplitudes in eqs. (3) following ref. [27]. In this reference the most general structure of a partial wave amplitude when the unphysical cuts are neglected was deduced. It was also shown that this structure is the one required in order to match with the tree level amplitudes calculated from the lowest order  $\chi PT$  Lagrangian [7] plus the exchange of the resonances [8], as in eqs. (3). In refs. [29, 30] the method is extended to include unphysical cuts as calculated in one loop  $\chi PT$  with and without baryons, respectively. For a review on these techniques, see ref. [31].

We work in the isospin limit. Our isospin states are:

$$\begin{aligned}
I &= 1 \\
|\pi\pi\rangle &= \frac{1}{2}|\pi^+\pi^- - \pi^-\pi^+\rangle \\
|K\bar{K}\rangle &= \frac{1}{\sqrt{2}}|K^+K^- - K^0\bar{K}^0\rangle \\
I &= 0 \\
|K\bar{K}\rangle &= \frac{1}{\sqrt{2}}|K^+K^- + K^0\bar{K}^0\rangle
\end{aligned} \tag{4}$$

note the extra factor  $1/\sqrt{2}$  in the normalization of the  $|\pi\pi\rangle$   $I = 1$  vector since in this state pions behave like identical particles. We have also removed a global  $e^{i\pi}$  phase in all the states in order to have the form factors positive defined in  $s = 0$ .

Since for  $I = 1$  we have two coupled channels, we will use in the following a matrix notation in which the pions are labeled by 1 and kaons by 2 in the  $I = 1$  case. For  $I = 0$  we have only the kaon channel which we denote by 1.

Taking into account eqs. (3) and (4) we can calculate for both isospin channels the tree level amplitudes between definite  $\pi\pi$  and  $K\bar{K}$  isospin states. We will collect these amplitudes, for each isospin channel, in a  $K_I$ -matrix. Thus, from ref. [27] we have the following expression for the  $T_I$ -matrix:

$$T_I(s) = [I + K_I(s) \cdot g^I(s)]^{-1} \cdot K_I(s) \tag{5}$$

where  $I$  is the unity matrix and  $g^I(s)$  is a diagonal matrix [27] given by the loop with two meson propagators. In dimensional regularization one has explicitly:

$$g_i^I(s) = \frac{1}{16\pi^2} \left[ -2 + d_i^I + \sigma_i(s) \log \frac{\sigma_i(s) + 1}{\sigma_i(s) - 1} \right] \quad (6)$$

where the subindex  $i$  refers to the corresponding two meson state and  $\sigma_i(s) = \sqrt{1 - 4m_i^2/s}$  with  $m_i$  the mass of the particles in the state  $i$ . For the choice  $d_i^I = 0$  one has  $g_i^I(s) = -\bar{J}(s)_{ii}$  with the  $\bar{J}(s)_{ii}$  functions defined in ref. [7] such that  $\bar{J}(0)_{ii} = 0$ .

We now introduce the diagonal matrix  $Q(s)_{ii} = p_i(s) \theta(s - 4m_i^2)$ , with  $p_i(s) = \sqrt{s/4 - m_i^2}$  the modulus of the c.m. three momentum of the state  $i$  and  $\theta(x)$  the usual Heaviside function. In terms of this matrix we have

$$S_I(s) = I + \frac{i}{4\pi\sqrt{s}} Q(s)^{1/2} \cdot T_I(s) \cdot Q(s)^{1/2} \quad (7)$$

with  $S_I(s)$  the  $S$ -matrix fulfilling the requirement  $S_I(s) \cdot S_I(s)^\dagger = I$ .

The electromagnetic meson form factor,  $F_{MM'}(s)$ , is introduced as follows. The transition amplitude from a photon, virtual or real, to a pair of mesons is written as:

$$\langle \gamma(q) | T | M(p) M'(p') \rangle = e \epsilon_\mu (p - p')^\mu F_{MM'}(s) \quad (8)$$

with  $q^2 = s$ ,  $e$  the modulus of the charge of an electron and  $\epsilon_\mu$  the photon polarization vector.

Unitarity of the  $S$ -matrix expressed between the  $\gamma$  and the  $MM'$  states, up to  $\mathcal{O}(e^2)$ , leads to the relationship:

$$p_{MM'}(s) \text{Im} F(s)_{MM'} = \sum_\alpha F_\alpha(s) \frac{p_\alpha(s)}{8\pi\sqrt{s}} p_\alpha(s) \theta(s - 4m_\alpha^2) (T_{\alpha,MM'}^{L=1}(s))^* \quad (9)$$

where  $*$  means complex conjugation and the strong amplitudes are projected in the P-wave. In the following we will remove the supraindex  $L = 1$  with the understanding that any strong amplitude will be in P-wave.

Dividing the former equation by  $p_{MM'}(s)$  and taking the complex conjugation of the term in the right hand side, since this is a real quantity above the threshold of the system  $|MM' \rangle$  where unitarity applies, one has:

$$\text{Im} F_{MM'}(s) = \sum_\alpha F_\alpha^*(s) \frac{p_\alpha(s)}{8\pi\sqrt{s}} \theta(s - 4m_\alpha^2) p_\alpha(s) \frac{T(s)_{\alpha,MM'}}{p_{MM'}(s)} \quad (10)$$

Taking into account that the  $T(s)_{\alpha\beta}$  is a symmetric matrix with respect indexes  $\alpha$  and  $\beta$  because of time reversal invariance, introducing also the diagonal matrix  $\tilde{Q}(s)_{ij} = p_i(s) \delta_{ij}$  and the one column matrix  $F(s)_i = F_i(s)$ , we can write eq. (10) in a matrix notation as:

$$\text{Im} F(s) = \tilde{Q}(s)^{-1} \cdot T(s) \cdot \frac{Q(s)}{8\pi\sqrt{s}} \cdot \tilde{Q}(s) \cdot F^*(s) \quad (11)$$

If we further substitute in the previous equation  $\text{Im} F(s)$  by  $(F(s) - F^*(s))/(2i)$  and  $T(s)$  by its expression in eq. (5), one finds:

$$F(s) = \left\{ I + \tilde{Q}(s)^{-1} \cdot [I + K(s) \cdot g(s)]^{-1} \cdot K(s) \cdot i \frac{Q(s)}{4\pi\sqrt{s}} \cdot \tilde{Q}(s) \right\} \cdot F^*(s)$$

$$\begin{aligned}
&= \tilde{Q}(s)^{-1} [I + K(s) \cdot g(s)]^{-1} \cdot \left\{ [I + K(s) \cdot g(s)] \cdot \tilde{Q}(s) + K(s) \cdot i \frac{Q(s)}{4\pi\sqrt{s}} \cdot \tilde{Q}(s) \right\} \cdot F^*(s) \\
&= \tilde{Q}(s)^{-1} \cdot [I + K(s) \cdot g(s)]^{-1} \cdot \tilde{Q}(s) \cdot \left\{ I + \tilde{Q}(s)^{-1} \cdot K(s) \cdot \tilde{Q}(s) \cdot g(s) \right. \\
&\quad \left. + \tilde{Q}(s)^{-1} \cdot K(s) \cdot \tilde{Q}(s) \cdot i \frac{Q(s)}{4\pi\sqrt{s}} \right\} \cdot F^*(s)
\end{aligned} \tag{12}$$

In the last equality we have made use of the fact that the matrices  $Q(s)$ ,  $\tilde{Q}(s)$  and  $g(s)$  commute since all of them are diagonal.

Let us first note that the symmetric matrix  $K(s)$ , eq. (3), is a matrix of functions with a kinematical cut in its  $K(s)_{12}$  matrix element between the threshold of channels 1 and 2 because  $K(s)_{12}$  is proportional to  $p_1(s)p_2(s)$ . However, the matrix  $\tilde{Q}(s)^{-1} \cdot K(s) \cdot \tilde{Q}(s)$  has no such kinematical cuts since the modulus of any of the three-momenta  $p_\alpha$  appears always squared. Note also that, although  $\tilde{Q}(s)^{-1}$  does not exist for  $s$  equal to its value for any of the thresholds, by continuity, the product  $\tilde{Q}(s)^{-1} \cdot K(s) \cdot \tilde{Q}(s)$  is well defined, and hence  $\tilde{Q}(s)^{-1} \cdot K(s) \cdot \tilde{Q}(s)$  is a well defined real matrix. Taking this into account and that

$$g(s)^* = g(s) + i \frac{Q(s)}{4\pi\sqrt{s}} \tag{13}$$

since

$$\text{Im}g(s) = -\frac{Q(s)}{8\pi\sqrt{s}}, \tag{14}$$

we can write eq. (12) as:

$$F(s) = \left[ I + \tilde{Q}(s)^{-1} \cdot K(s) \cdot \tilde{Q}(s) \cdot g(s) \right]^{-1} \cdot \left[ I + \tilde{Q}(s)^{-1} \cdot K(s) \cdot \tilde{Q}(s) \cdot g^*(s) \right] \cdot F^*(s) \tag{15}$$

Multiplying both sides of the former equation by  $\left[ I + \tilde{Q}(s)^{-1} \cdot K(s) \cdot \tilde{Q}(s) \cdot g(s) \right]$  we arrive at the interesting result:

$$\left[ I + \tilde{Q}(s)^{-1} \cdot K(s) \cdot \tilde{Q}(s) \cdot g(s) \right] \cdot F(s) = \left[ I + \tilde{Q}(s)^{-1} \cdot K(s) \cdot \tilde{Q}(s) \cdot g^*(s) \right] \cdot F^*(s) \tag{16}$$

This implies that the matrix  $\left[ I + \tilde{Q}(s)^{-1} \cdot K(s) \cdot \tilde{Q}(s) \cdot g(s) \right] \cdot F(s)$  has no cuts at all, since the right hand cut or unitarity cut, the only one present in  $g(s)$  or  $F(s)$ , has been removed. Note that, as it is well known, a form factor is an analytic function of  $s$  except for the presence of the right hand cut from threshold up to infinity. It can also have poles on the real  $s$  axis below threshold, corresponding to bound states, and poles in the complex plane in the unphysical Riemann sheets corresponding to resonances. On the other hand, as discussed above in contrast to  $K(s)$ ,  $\tilde{Q}(s)^{-1} \cdot K(s) \cdot \tilde{Q}(s)$  is a function free of physical or kinematical cuts. From eq. (16) we write now

$$\begin{aligned}
F(s) &= \left[ I + \tilde{Q}(s)^{-1} \cdot K(s) \cdot \tilde{Q}(s) \cdot g(s) \right]^{-1} \cdot R(s) \\
&= \tilde{Q}(s)^{-1} \cdot [I + K(s) \cdot g(s)]^{-1} \cdot \tilde{Q}(s) \cdot R(s)
\end{aligned} \tag{17}$$

with  $R(s)$  a function free of any cut. Note also that the matrix  $D(s) \equiv I + K(s) \cdot g(s)$  was already introduced in eq. (5) in relation with the purely strong  $T$ -matrix.

As told above, the considered large  $N_c$  leading contributions are given in eqs. (2). In fact in this limit  $D(s) = I + \mathcal{O}(N_c^{-1})$  and hence we have:

$$F(s) = R(s)_{N_c \text{ leading}} = F^t(s) \quad (18)$$

where  $F^t(s)$  is the tree level form factor. As a result we can write:

$$R(s) = F^t(s) + \delta R(s) \quad (19)$$

with  $\delta R(s)$  subleading in large  $N_c$  and free of any cut. Since the pole singularities present in the form factor correspond to tree level resonances (already present in  $F^t(s)$ ) or dynamically generated resonances from the  $D(s)$  matrix, see eqs. (17) and (5), the  $\delta R(s)$  matrix should then be simply a matrix made up of polynomials<sup>3</sup>.

Hence, we can rewrite eq. (17) as:

$$F(s) = \left[ I + \tilde{Q}(s)^{-1} \cdot K(s) \cdot \tilde{Q}(s) \cdot g(s) \right]^{-1} \cdot [F^t(s) + \delta R(s)] \quad (20)$$

We can further reduce eq. (20) for the two channel case. Indeed, given the structure of the  $K$  matrix of eq (3) for  $I = 1$  and  $\pi\pi$  and  $K\bar{K}$  channels we find

$$F(s) = \frac{1}{\det[D(s)]} \begin{pmatrix} 1 + p_2(s)^2 \beta(s) g_2^1(s) & -\sqrt{2} p_2(s)^2 \beta(s) g_2^1(s) \\ -\sqrt{2} p_1(s)^2 \beta(s) g_1^1(s) & 1 + 2 p_1(s)^2 \beta(s) g_1^1(s) \end{pmatrix} (F^t(s) + \delta R(s)) \quad (21)$$

with  $\beta$  given by

$$\beta(s) = \frac{1}{3f^2} \left( 1 + \frac{2G_V^2}{f^2} \frac{s}{M_\rho^2 - s} \right) \quad (22)$$

and  $\det[D(s)] = 1 + 2p_1(s)^2 \beta(s) g_1^1(s) + p_2(s)^2 \beta(s) g_2^1(s)$ . For  $I = 0$ , with only one channel, eq. (20) is simple enough. In the explicit formula of eq. (21) we can see that there are indeed no kinematical cuts associated to the  $p_1 p_2$  factors of the matrix  $K$ , as argued above.

The unitarity method we have introduced is similar to the one discussed in ref. [32] in order to solve the Muskhelishvili-Omnès problem [15]. The differences arise from the fact that we have showed how to deal with the kinematical singularities associated with the product  $p_i \text{Im} F(s)_i$  eq. (9), and also because we have allowed the presence of pole singularities both in  $D(s)$ , due to  $K(s)$ , and in  $\tilde{F}(s)$ . However, they appear in such a way that they cancel each other and the results are finite. In that reference [32] the connection between eq. (20) and an Omnès representation for the elastic case is also discussed. This relation is easily seen since in the elastic case  $D^{-1}(s)$  has the phase of the strong scattering amplitude, eq. (5), and only has the right hand cut. There is, however, a subtle point which is that  $D^{-1}(s)$  has zeros for  $s$  equal to the bare masses of the vector resonances introduced in  $K(s)$  and they have to be removed in order to make an Omnès representation. This is accomplished automatically in eq. (20) due to the explicit presence of the bare resonance poles in  $F^t(s)$ .

The degree of the polynomials present in  $\delta R(s)$  can be restricted when considering the behavior of the form factors in the limit  $s \rightarrow \infty$ . In fact from eqs. (2), (3) and (20) we have the following limits:

---

<sup>3</sup>It should be understood in the former sentence that subleading corrections in  $1/N_c$  to the couplings and masses of the resonances (not coming in our formalism by the  $D(s)$  function), have to be reabsorbed in a renormalization of  $F^t(s)$ , eq. (2).



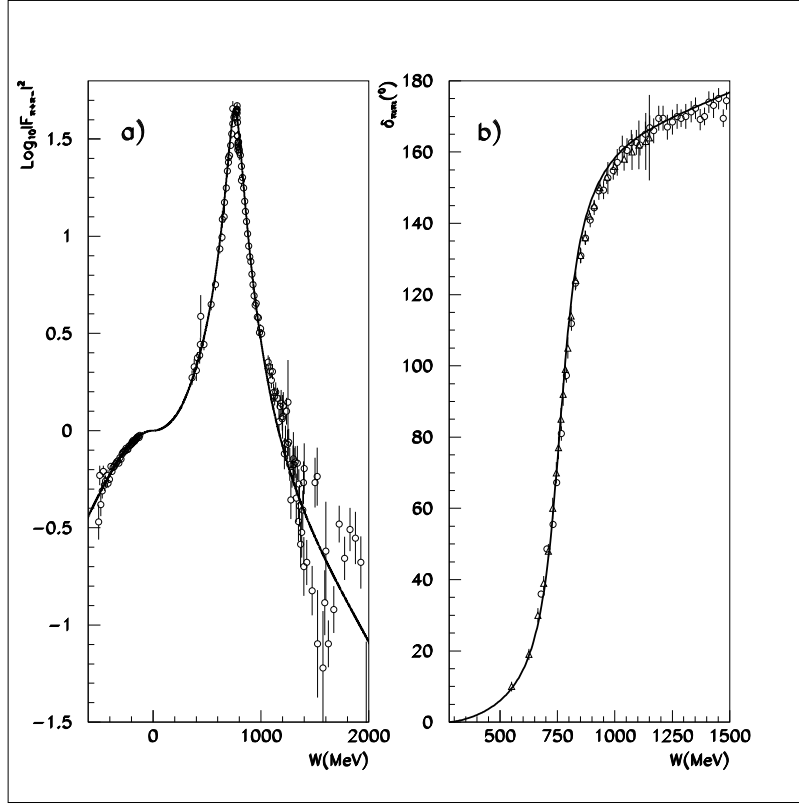


Figure 3:  $W$  is defined as  $\sqrt{s}$  for  $s > 0$  and as  $-\sqrt{-s}$  for  $s < 0$ . From left to right: a)  $\pi^+\pi^-$  vector form factor. Experimental data from ref. [4] collecting also data from refs. [38] for positive  $s$ . For negatives  $s$  ref. [39] b)  $\pi\pi$  P-wave phase shifts. Triangles from ref. [40] and circles from ref. [41]

$$\begin{aligned}
& I=1 \\
F_1(\infty) &= \frac{1 - \frac{F_V G_V}{f^2} + \delta R_1^1(\infty) + g_2^1(\infty) \frac{s}{12f^2} (1 - \frac{2G_V^2}{f^2}) [\delta R_1^1(\infty) - \sqrt{2}\delta R_2^1(\infty)]}{1 + \frac{s}{6f^2} (1 - \frac{2G_V^2}{f^2}) \{g_1^1(\infty) + \frac{1}{2}g_2^1(\infty)\}} \\
F_2(\infty) &= \frac{1 - \frac{F_V G_V}{f^2} + \sqrt{2}\delta R_2^1(\infty) + g_1^1(\infty) \frac{s}{6f^2} (1 - \frac{2G_V^2}{f^2}) [\sqrt{2}\delta R_2^1(\infty) - \delta R_1^1(\infty)]}{\sqrt{2} + \frac{\sqrt{2}s}{6f^2} (1 - \frac{2G_V^2}{f^2}) \{g_1^1(\infty) + \frac{1}{2}g_2^1(\infty)\}} \\
& I=0 \\
F_1(\infty) &= \frac{1 - \frac{F_V G_V}{f^2} + \sqrt{2}\delta R_1^0(\infty)}{\sqrt{2} + \frac{\sqrt{2}s}{4f^2} (1 - \frac{2G_V^2}{f^2}) g_1^0(\infty)} \tag{23}
\end{aligned}$$

where  $g_i^I(\infty)$  is a quantity logarithmically divergent with  $s \rightarrow \infty$ , see eq. (6). We denote by  $\delta R_i^I(\infty)$  the value of the vector element of  $\delta R(s)$  with isospin  $I$  and channel  $i$  for  $s \rightarrow \infty$ . Clearly, this value diverges as  $s^{n(I;i)}$  with  $n(I;i)$  the degree of the polynomial  $\delta R_i^I(\infty)$ .

From perturbative QCD [33], it is known that the vector pion form factor goes at most as a constant for  $s \rightarrow \infty$ . Although experimentally, and also from the quark counting

rules, it is very likely that it vanishes for  $s \rightarrow \infty$ . Experimentally, we have  $F_V = 154$  MeV from the observed decay rate  $\Gamma(\rho^0 \rightarrow e^+e^-)$  [8] and  $G_V = 53$  MeV from a study of the pion electromagnetic radii after taking into account corrections from chiral loops at next to leading order [7]. With these values, we see from eqs. (23) for the  $I = 0$  case, that  $\delta R_1^0(s)$  can have, at most, degree one since otherwise the form factor would be divergent (we are assuming here that the high energy limit of the kaon form factors is the same as the aforementioned one of the pion vector form factor). Analogously for  $I = 1$ , we see that the difference  $\delta R_1^1(s) - \sqrt{2}\delta R_2^1(s)$  can be at most a constant, while, independently,  $\delta R_i^1(s)$  can have degree one. If we further require that the vector form factors vanish for  $s \rightarrow \infty$ , both for the pion and kaon ones, then  $\delta R_i^I(s)$  are constants and

$$\delta R_1^1 = \sqrt{2}\delta R_2^1. \quad (24)$$

In the following we will assume that this is the case<sup>4</sup>. Note that since  $\delta R_i^1(s)$  are at least  $\mathcal{O}(p^2)$  quantities, these constants must be proportional to the square of the pseudoscalar masses  $m_\pi^2, m_K^2$ . Then we will finally have:

$$F(s) = \left[ I + \tilde{Q}(s)^{-1} \cdot K(s) \cdot \tilde{Q}(s) \cdot g(s) \right]^{-1} \cdot (F^t(s) + \alpha_I) \quad (25)$$

where  $\alpha_I$  is just a constant for  $I = 0$  and for  $I = 1$ , taking into account eq. (24),  $\alpha_1$  can be written as:

$$\begin{pmatrix} \alpha'_1 \\ \alpha'_1/\sqrt{2} \end{pmatrix} \quad (26)$$

with  $\alpha'_1$  a constant.

### 3.1 Matching with one loop $\chi PT$

In order to fix the values of the constants  $d_i^I$  of  $g_i^I(s)$  and  $\alpha_I$  of eq. (25) we match our results with those of  $\chi PT$  up to one loop [7]. The form factors from [7], together with eq. (4) for the definition of the isospin states, are:

$$\begin{aligned} F_{\pi\pi}^{I=1} &= 1 + 2H_{\pi\pi} + H_{KK} \\ F_{K\bar{K}}^{I=1} &= \frac{1}{\sqrt{2}}(1 + 2H_{\pi\pi} + H_{KK}) \\ F_{K\bar{K}}^{I=0} &= \frac{1}{\sqrt{2}}(1 + 3H_{KK}) \end{aligned} \quad (27)$$

with the function  $H_{ii}(s)$  given by:

$$H_{ii}(s) = \frac{2s}{3f^2}L_9^r(\mu) + \frac{s}{192\pi^2 f^2} \left( 2\sigma_i(s)^2 - \sigma_i^3(s) \log \frac{\sigma_i(s) + 1}{\sigma_i(s) - 1} - \frac{1}{3} + \log \frac{\mu^2}{m_i^2} \right) \quad (28)$$

In order to make the matching with the one loop  $\chi PT$  form factors, we will take into account the fact that for evaluating the contribution of the octet of vector resonances to the  $\mathcal{O}(p^4)$   $\chi PT$  counterterms, for instance to  $L_9^r(\mu)$ , the masses of these resonances have to

---

<sup>4</sup>We refer the reader to refs. [34, 8] which stress the importance to keep the short distance QCD constraints in order to guarantee the independence of the results under spin-1 field redefinitions.

be taken in the chiral limit [8]. We will denote this mass in the following by  $M_V \approx M_\rho$  [8]. As noted in ref. [8] the  $L_9^r(\mu)$  is saturated by the meson vector resonance exchanges at a scale  $\mu$  around the mass of the  $\rho$ , such that

$$2L_9(\mu \approx M_\rho^{physical}) = \frac{F_V G_V}{M_V^2} \quad (29)$$

we will also make use of this result in the following.

Let us consider first the  $I = 1$  case. Expanding our results, eq. (25), up to one loop in the  $\chi PT$  counting, we have:

$$\begin{aligned} F_{\pi\pi}^{I=1}(s) &= 1 + \alpha'_1 + \frac{F_V G_V s}{M_V^2 f^2} + \frac{s}{96\pi^2 f^2} \left\{ 2\sigma_\pi(s)^2 - \sigma_\pi(s)^2 d_1^1 - \sigma_\pi(s)^3 \log \frac{\sigma_\pi(s) + 1}{\sigma_\pi(s) - 1} \right\} + \\ &+ \frac{s}{192\pi^2 f^2} \left\{ 2\sigma_K(s)^2 - \sigma_K(s)^2 d_2^1 - \sigma_K(s)^3 \log \frac{\sigma_K(s) + 1}{\sigma_K(s) - 1} \right\} \end{aligned} \quad (30)$$

while the one loop  $\chi PT$  result is:

$$\begin{aligned} F_{\pi\pi}^{I=1}(s) &= 1 + \frac{2L_9^r(\mu)s}{f^2} + \frac{s}{96\pi^2 f^2} \left\{ 2\sigma_\pi(s)^2 - \sigma_\pi(s)^3 \log \frac{\sigma_\pi(s) + 1}{\sigma_\pi(s) - 1} - \frac{1}{3} - \log \frac{m_\pi^2}{\mu^2} \right\} + \\ &+ \frac{s}{192\pi^2 f^2} \left\{ 2\sigma_K(s)^2 - \sigma_K(s)^3 \log \frac{\sigma_K(s) + 1}{\sigma_K(s) - 1} - \frac{1}{3} - \log \frac{m_K^2}{\mu^2} \right\} \end{aligned} \quad (31)$$

The matching for  $K\bar{K}$  form factor in  $I = 1$  does not give any new condition since this form factor, at the one loop chiral level, is simply  $1/\sqrt{2}$  of the  $\pi\pi$  one, both in our approach and in  $\chi PT$  [7]. Note that this happens independently of the value of the constant  $\alpha'_1$ , because of eq. (26).

In the following we will take

$$\alpha'_1 = 0 \quad (32)$$

in order to constraint further our approach. This can be done since, as we show below, we can match our results with one loop  $\chi PT$  by choosing appropriate values for  $d_1^1$  and  $d_2^1$ . On the other hand, as we will see in the next section, a very nice description of the pion form factor and of the  $\pi\pi$  P-wave phase shifts, see fig. 3, is given without including this extra degree of freedom. In addition, we will discuss below the sensitivity of our results under changes of  $\alpha'_1 \neq 0$ .

By matching eqs. (30) and (31) with  $\alpha'_1 = 0$ , taking also into account eq. (29), one finds the condition:

$$\sigma_\pi(s)^2 d_1^1 + \frac{\sigma_K(s)^2}{2} d_2^1 = \frac{1}{2} + \log \frac{m_\pi^2}{\mu^2} + \frac{1}{2} \log \frac{m_K^2}{\mu^2} \quad (33)$$

Identifying the terms independent of  $s$  and linear in  $1/s$ , we finally have:

$$\begin{aligned} d_1^1 &= \frac{m_K^2}{m_K^2 - m_\pi^2} \left( \log \frac{m_\pi^2}{\mu^2} + \frac{1}{2} \log \frac{m_K^2}{\mu^2} + \frac{1}{2} \right) \\ d_2^1 &= \frac{-2 m_\pi^2}{m_K^2 - m_\pi^2} \left( \log \frac{m_\pi^2}{\mu^2} + \frac{1}{2} \log \frac{m_K^2}{\mu^2} + \frac{1}{2} \right) \end{aligned} \quad (34)$$

Next we do the matching in the  $I = 0$  sector. Our chiral one loop expression for this form factor is:

$$\sqrt{2}F_{K\bar{K}}^{I=0} = 1 + \sqrt{2}\alpha_0 + \frac{F_V G_V s}{M_V^2 f^2} + \frac{s}{64\pi^2 f^2} \left\{ 2\sigma_K(s)^2 - d_1^0 \sigma_K(s)^2 - \sigma_K(s)^3 \log \frac{\sigma_K(s) + 1}{\sigma_K(s) - 1} \right\} \quad (35)$$

The  $\chi PT$  one is:

$$\sqrt{2}F_{K\bar{K}}^{I=0} = 1 + \frac{2s}{f^2} L_9^r(\mu) + \frac{s}{64\pi^2 f^2} \left\{ 2\sigma_K(s)^2 - \sigma_K(s)^3 \log \frac{\sigma_K(s) + 1}{\sigma_K(s) - 1} - \frac{1}{3} - \log \frac{m_K^2}{\mu^2} \right\} \quad (36)$$

By matching eqs. (35) and (36), taking also into account eq. (29), we obtain the condition:

$$\sqrt{2}\alpha_0 - \frac{s\sigma_K(s)^2 d_1^0}{64\pi^2 f^2} = -\frac{s}{64\pi^2 f^2} \left( \frac{1}{3} + \log \frac{m_K^2}{\mu^2} \right) \quad (37)$$

Identifying the terms independent of  $s$  and those linear in  $s$ :

$$\begin{aligned} d_1^0 &= \frac{1}{3} + \log \frac{m_K^2}{\mu^2} \\ \alpha_0 &= -\frac{m_K^2}{16\sqrt{2}\pi^2 f^2} \left( \frac{1}{3} + \log \frac{m_K^2}{\mu^2} \right) \end{aligned} \quad (38)$$

We see indeed that  $\alpha_0$  is subleading in  $N_c$  since  $f^2 \sim N_c$  and  $m_K^2 \sim 1$  in this counting. Numerically we find it to be of the order of 0.1 for  $\mu = M_\rho$ , consistent with the large  $N_c$  counting.

## 4 Results

Once we have fixed the constants  $d_i^I$  and  $\alpha_I$  by eqs. (32), (34) and (38), our final expression, eq. (25), for the vector form factors only depends on the bare masses of the  $\rho$ ,  $\phi$  and  $\omega$  resonances and on the couplings  $G_V$  and  $F_V$  and on  $f$ . The couplings  $F_V$  and  $G_V$  are fixed, as explained in section 3, from their experimental values, 154 MeV and 53 MeV, respectively. The value for the parameter  $f$  is taken from the second entry of ref. [7], where it is derived by working out the relation of the ratio  $f_\pi/f$  with the isoscalar  $\bar{u}u + \bar{d}d$  radius of the pion. The resulting central value is  $f = 87.4$  MeV. Notice that this estimate is done for the value of  $f$  in the limit  $m_u = m_d = 0$  and  $m_s \neq 0$  and there is some controversy about the possible deviations with respect this value when considering the  $SU(3)$  case [35, 36]. The bare masses can be fixed in terms of  $F_V$ ,  $G_V$  and  $f$  by the requirements that the moduli of the  $\pi\pi$   $I = 1$  and  $K\bar{K}$   $I=0$  P-wave amplitudes have a maximum for  $\sqrt{s} = M_\rho^{physical} = 770$  MeV and for  $\sqrt{s} = M_\phi^{physical} = 1019.413$  MeV, respectively. We obtain the values  $M_\rho = 829.8$  MeV and  $M_\phi = 1026.581$  MeV, where the number of decimals correspond to the experimental precision in which the physical masses are given [37].

For the mass of the  $\omega$  we take directly 782 MeV since there are no experimental data in the region of the  $\omega$  and its contributions to other physical regions do not depend on such fine details since the  $\omega$  is very narrow.

Finally, note that our physical results does not depend on the regularization scale  $\mu$  since any change in the scale is reabsorbed by the corresponding change in the constants  $d_i^I(\mu)$ . However, since we have made use of eq. (29), we have to consider a value for  $\mu$  around the mass of the  $\rho$  meson, where vector meson saturation of the  $L_i^r(\mu)$  coefficients works [8]. In the following we will fix  $\mu = M_\rho$ .

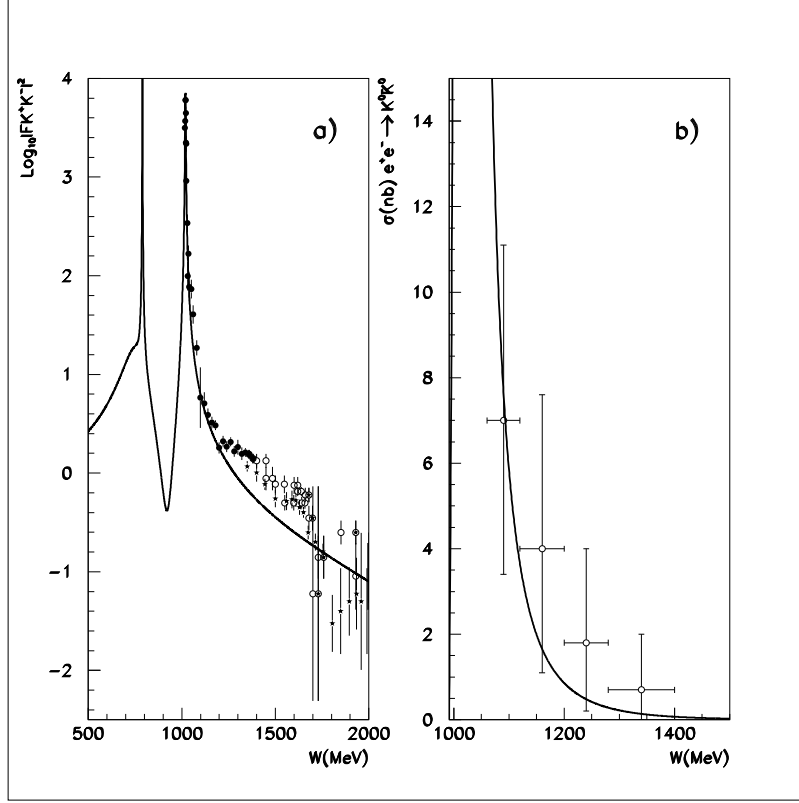


Figure 4:  $W$  is defined as  $\sqrt{s}$  for  $s > 0$  and as  $-\sqrt{-s}$  for  $s < 0$ . From left to right: a)  $K^+K^-$  vector form factor. Experimental data: black circles [42], white circles [43] and stars [44]. b)  $\sigma(e^+e^- \rightarrow K^0\bar{K}^0)$  in nb. Data: [45]

As can be seen in figs. 3, 4 and 5, we can describe in a very precise way the vector pion and kaon form factors from negative values of  $s$  up to about  $1.44 \text{ GeV}^2$ . The P-wave  $\pi\pi$  phase shifts are also very well reproduced even for energies higher than those for the form factors, fig. 3 is displayed until  $\sqrt{s} = 1.5 \text{ GeV}$ . Note that the curves present in those figures do not result from a fit making use of our approach since the parameters have been fixed in advance. Furthermore, the qualitative behavior of the data for the form factors is reproduced even for very high energies. For values of  $\sqrt{s}$  higher than  $1.2 \text{ GeV}$  new effects appear: 1) the presence of more massive resonances,  $\rho'$ ,  $\omega'$ ,  $\phi'$ ... These states can be in principle taken into account by our formalism just by adding more resonance to eqs. (2) and (3). 2) More seriously and less trivial is taking into account the effect due to multiparticle states, e.g.  $4\pi$ ,  $\omega\pi$  ... In fact, since in our model the widths of the resonances are derived dynamically in terms of the included channels we cannot mimic the effect of such multiparticle states as done in other studies in which the widths of the resonances are fitted, that is, incorporated by hand. This is currently done when using parameterizations of the type of ref. [3, 4]. In fact, in the present case we have found that the effect of other

channels cannot be neglected for energies higher than  $\sqrt{s} \gtrsim 1.2$  GeV, for which we do not give a fair reproduction of all the structures present in the data. We have checked that the inclusion of higher mass resonances like the  $\rho'$  improves the agreement with the data but there are clear signs that other elements are still missing.

In fig.4a one clearly sees the peaks of the  $\phi$ ,  $\rho$  and  $\omega$  resonances, the latter on the top of the  $\rho$ . The  $\omega$  peak corresponds to that of a zero width resonance since it appears below the  $K\bar{K}$  threshold and the  $3\pi$  state is not included.

In figs.5a,b we compare for low energies our results for the pion and charged kaons vector form factors with the results obtained in  $\chi PT$  for the pion vector form factor, up to one [7] and two loops [13, 14], and with the one loop  $\chi PT$  [7] charged kaon vector form factor. In the figures the aforementioned matching, guaranteed by construction, is clearly seen, and the resummation accomplished by eq. (25) provides the right corrections to the  $\chi PT$  results also for low energies. In fact, we see a much better agreement of our result with the two loop  $\chi PT$  pion vector form factor than with the one loop result.

In table 1 we give the calculated electromagnetic radii of the pions, charged and neutral kaons and compare them with one loop  $\chi PT$  [7] and with experiment. We have not shown the two loop  $\chi PT$  value for  $\langle r_\pi^2 \rangle$  since its experimental value [48] is taken as an input in order to fix a counterterm [13]. In ref. [14] it is argued that this is a sensible assumption within an accuracy around a 10% in the value of  $\langle r^2 \rangle_V^\pi$ . Our results for pions and charged kaons are compatible with the  $\chi PT$  results and experiment within errors. For the case of neutral kaons, assuming as we have, the same uncertainties as in the  $\chi PT$  results, we are also compatible with experiment. It is also interesting to compare our values for the electromagnetic radii with a low energy theorem due to Sirlin [51]. This theorem states that,

$$\mathcal{O}[(m_s - \hat{m})^2] = \frac{1}{2} \left( F_V^\pi(s) + F_V^{K^+}(s) \right) + F_V^{K^0}(s) - f_+^{K\pi}(s) \quad (39)$$

where  $m_s$  is the mass of the strange quark,  $\hat{m}$  is the average between the masses of the up and down quarks and  $f_+^{K\pi}$  is one piece of the vector  $K\pi$  form factor [7]. In the previous relation the contribution of heavy quarks have been neglected and we follow the notation of ref. [7]. Numerically at  $\mathcal{O}(p^4)$  in  $\chi PT$  [7] one has, for the same combination of electromagnetic radii as in the right hand side of eq. (39),  $0.00 \pm 0.05 \text{ fm}^2$ . At  $\mathcal{O}(p^6)$  the result is [52]  $0.021 \pm 0.003 \text{ fm}^2$ . From the values shown in table 1, taking from experiment the electromagnetic radius  $\langle r^2 \rangle_V^{K\pi} = 0.36 \pm 0.02 \text{ fm}^2$  [37], as also done in  $\mathcal{O}(p^4)$   $\chi PT$ , we have  $-0.07 \pm 0.05 \text{ fm}^2$ . The experimental value, from refs. [47, 49, 50, 37], is  $-0.02 \pm 0.05 \text{ fm}^2$ .

In figs.5c,d the resonance regions for the  $\rho$  and  $\phi$  mesons are shown in detail. In the case of the pion form factor in the  $\rho$  region, we have compared our results with the experimental data of ref. [21] since in  $\tau$  decays only the  $I = 1$  part of the pion form factors plays a role and we are working in the isospin limit. As can be seen the reproduction of data is very good in both cases.

As announced before, we have also studied the dependence of the results on the sub-leading constant  $\alpha'_1$  which has been set to zero in eq. (32). Notice that the matching to  $\chi PT$  gives new values for the  $d_I^1$  parameters in terms of those of  $\alpha'_1$  and also one has to recalculate the bare mass of the  $\rho$  resonance. The new results, obtained with reasonable values of  $\alpha'_1$ , can be hardly distinguished from the  $\alpha'_1 = 0$  case in the region  $\sqrt{s} < 1.2$  GeV. A fit to the  $\pi\pi$  phase shifts and the form factors data gives that the best values are  $\alpha'_1 = -0.0012$  and  $M_\rho = 830.23 \text{ MeV}$ , leading to results that are indistinguishable from the ones obtained by setting  $\alpha'_1 = 0$ .

Finally, in our approach we have taken into account  $\pi\pi$  and  $K\bar{K}$  coupled channels for

the  $I = 1$  P-wave. The effect of coupled channels is more important for kaons, particularly for the neutral ones, than for pions. This can be expected since when we decouple the kaons from the pions the  $\rho$  resonance appears in the kaon vector form factors as a zero width resonance and this is a very bad approximation, particularly, if we are interested around the rather broad  $\rho$  energy region. On the other hand, around the peak of the  $\phi$  the effect of the pions is small, of the order of a few percent, and the kaon vector form factor is dominated by the  $K\bar{K}$  elastic channel strongly coupled to the  $\phi$ . However, as we move again to higher energies, where the form factors have dropped substantially, the pion channels become again important.

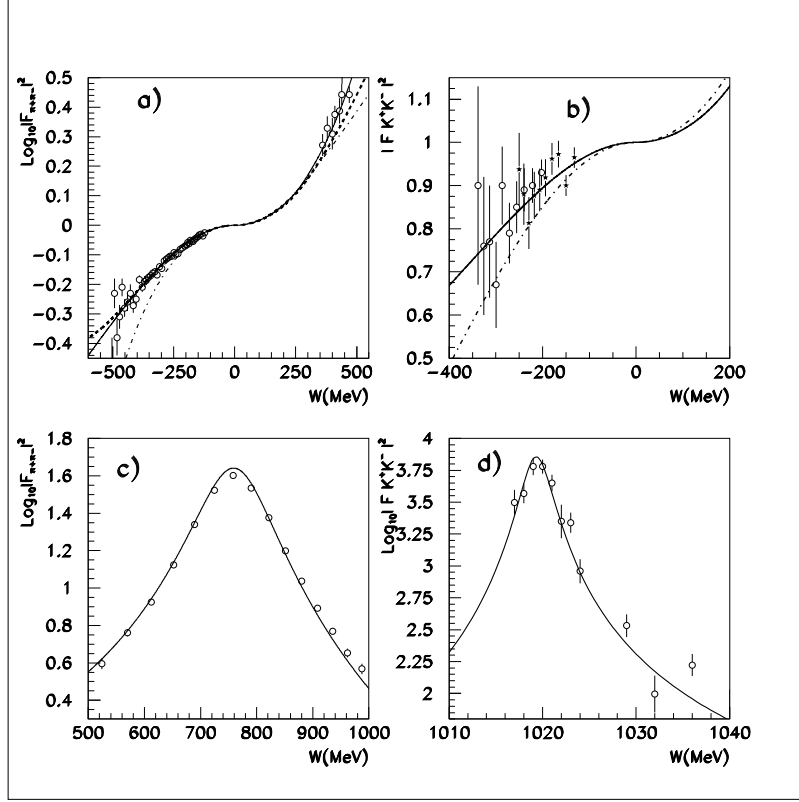


Figure 5:  $W$  is defined as  $\sqrt{s}$  for  $s > 0$  and as  $-\sqrt{-s}$  for  $s < 0$ . From left to right and top to bottom: a) Vector pion form factor. The dashed-dotted line represents one loop  $\chi PT$  ref. [7] and the dashed one the two loop  $\chi PT$  result ref. [14]. b)  $K^+K^-$  form factor. The meaning of the lines is the same as before. Data are from ref. [46], white circles, and the star points are from ref. [47]. c) Vector pion form factor in the  $\rho$  region without taking into account the  $\rho - \omega$  mixing effect. Data from  $\tau$ -decays [21]. d)  $K^+K^-$  form factor. Data [42].

#### 4.1 Isospin violation: $\rho - \omega$ mixing.

The incorporation of isospin violation effects, due to the mass differences from the  $u$  and  $d$  quarks and electromagnetic corrections, is readily possible, up to some extend, within the present formalism. As an example, consider the OZI violating process  $\phi \rightarrow \pi^+\pi^-$  studied in ref. [53] within a chiral unitary approach. It was noted there that the  $\omega \rightarrow \pi^+\pi^-$  decay requires a direct  $\rho - \omega$  mixing which makes this process qualitatively different to

e.m. radii (fm <sup>2</sup> )	Our results	One loop $\chi PT$	Experiment
$\langle r^2 \rangle_V^\pi$	0.44	$0.44 \pm 0.04$	$0.439 \pm 0.030$ [50]
$\langle r^2 \rangle_V^{K^+}$	0.34	$0.38 \pm 0.03$	$0.34 \pm 0.05$ [47] $0.28 \pm 0.07$ [46]
$\langle r^2 \rangle_V^{K^0}$	-0.10	$-0.04 \pm 0.03$	$-0.054 \pm 0.026$ [49]

Table 1: Electromagnetic radii for  $\pi^+\pi^-$ ,  $K^+K^-$  and  $K^0\overline{K}^0$ , from left to right respectively. In the table are given our results, the ones from  $\chi PT$  at next-to-leading order ref. [7] and some experimental data. The uncertainty in our values has to be considered of the same size than the one in  $\chi PT$ , that is, around  $\pm 0.04$  fm<sup>2</sup>.

the  $\phi \rightarrow \pi^+\pi^-$ . This  $\rho - \omega$  mixing has been studied in the context of chiral Lagrangians, together with the large  $N_c$  expansion, in [54] with the result:

$$i\mathcal{L} \rightarrow i\frac{1}{2}\tilde{\Theta}_{\rho\omega}\rho_{\mu\nu}^0\omega^{\mu\nu} \quad (40)$$

with

$$\tilde{\Theta}_{\rho\omega} = -(m_{K^0}^2 - m_{K^+}^2) + (m_{\pi^0}^2 - m_{\pi^+}^2) + \frac{e^2 F_V^2}{3} \quad (41)$$

Given the smallness of the contribution from  $\rho - \omega$  mixing one can add to the result for the pion form factor evaluated before the contribution from the mechanism of fig.6.

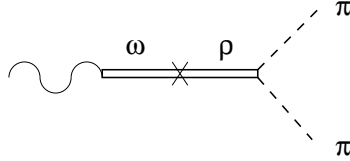


Figure 6: Feynman diagram corresponding to the  $\rho - \omega$  mixing contribution to the pion form factor.

The contribution of fig.6 is straightforward and has been evaluated previously in [20]. With the  $\gamma\omega$  and  $\rho\pi\pi$  couplings from [8] and the  $\rho - \omega$  coupling of eq. (40) we obtain:

$$\Delta F = -\frac{1}{3}\frac{F_V G_V}{f^2}s \frac{1}{s - M_\omega^2 + i\sqrt{s}\Gamma_\omega(s)} \frac{1}{s - M_\rho^2 + i\sqrt{s}\Gamma_\rho(s)} \tilde{\Theta}_{\rho\omega} \quad (42)$$

Since this correction is only visible around the  $\rho$  peak we take for  $\Gamma_\omega(s)$ ,  $\Gamma_\rho(s)$  the constant values of the PDG [37] (using instead an energy dependence width of the  $\rho$  meson does not introduce any appreciable effects).

With a value for  $\tilde{\Theta}_{\rho\omega}$  of  $-4500$  MeV<sup>2</sup> from eq. (41), which is also consistent with empirical determinations [55, 56], we get the form factor shown in fig.7 which reproduces fairly well the experimental data at the peak of the pion form factor. It is worth mentioning that this effect of isospin violation is not observed in the data from  $\tau$  decay since this process is only sensitive to the  $I = 1$  current (see fig.5).



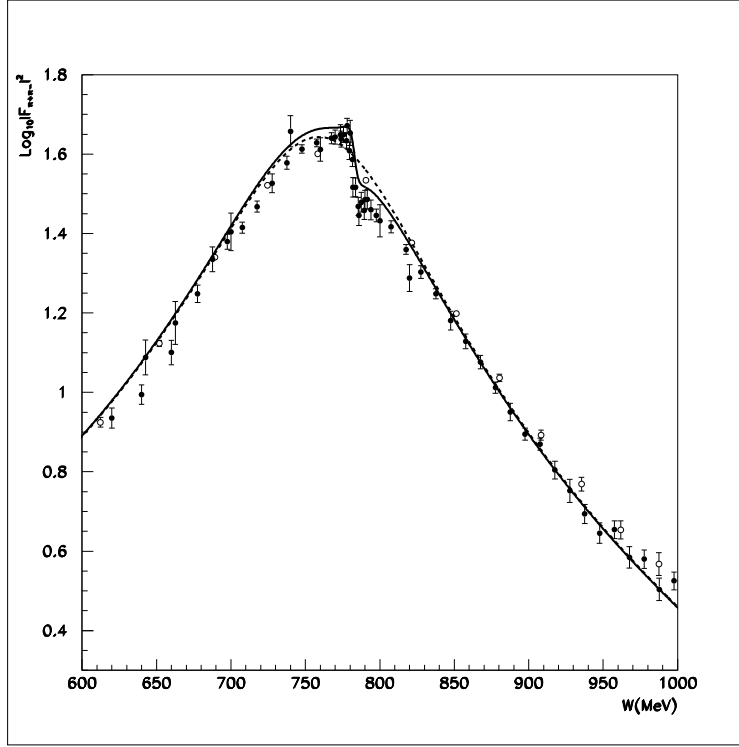


Figure 7: Solid line: pion vector form factor taking into account the  $\rho - \omega$  mixing; dashed line:  $I=1$  vector form factor in the isospin limit. Data: black circles from  $e^+e^- \rightarrow \pi^+\pi^-$  reactions [4, 38]; white circles: data from  $\tau$ -decays [21].

## 5 Conclusions

We have developed an appropriate method to take into account the final state interaction corrections to the tree level amplitudes of refs. [7, 8] with explicit resonance fields.

The strong tree level scattering amplitudes from refs. [7, 8] were unitarized in coupled channels following the scheme developed in ref. [27]. These amplitudes were then implemented in order to derive the final state corrections to the tree level vector form factors, eqs. (2). As a result a very good description of data is accomplished for  $\sqrt{s} \lesssim 1.2$  GeV. For higher energies multiparticle channels are no longer negligible and also new resonances appear, although our results still give the trend of the experimental data.

Our expressions reproduce the  $\chi PT$  expansion of the pion and kaon vector form factors up to one loop [7]. The resummation of our scheme leads, in the low energy region where  $\chi PT$  is expected to hold (see fig.5a), to a much better agreement with the two loop  $\chi PT$  pion vector form factor than with the one loop one. However, at the same time, we are able to provide a very good description at higher energies, including the resonance regions where standard  $\chi PT$  could not be applied, figs. 5c and 5d. Furthermore, our calculated electromagnetic radius of the  $\pi^+$ ,  $K^+$  and  $K^0$ , table 1, are in agreement with experiment, assuming the same uncertainties as in the  $\chi PT$  results.

We have also taken into account the  $\rho - \omega$  mixing as a main source of isospin breaking in order to compare our results with the form factor obtained from  $e^+e^- \rightarrow \pi^+\pi^-$ . The input for the  $\rho - \omega$  mixing has been taken from recent work respecting also chiral symmetry

in the same line as the rest of the Lagrangians employed here.

Finally, our method also provides P-wave scattering amplitudes for pions and kaons in very good agreement with the experimental data on the phase shifts for the former one. For the case of the kaons there are no scattering data available, but they would be highly desirable as a further test of the chiral unitary approach followed here.

## Acknowledgments

We would like to acknowledge useful discussions and a critical reading by Ulf-G. Meißner. Multiple and useful discussions with A. Pich are also acknowledged. We also thank J. Portolés for calling our attention to ref. [34]. Partial financial support from the DGICYT under contract PB96-0753 and from the EU TMR network Eurodaphne, contract no. ERBFMRX-CT98-0169 is acknowledged as well. J.E.P. thanks financial support from the Ministerio de Educación y Cultura.

## References

- [1] J. J. Sakurai, *Currents and Mesons*, University of Chicago Press, Chicago, 1969.
- [2] G. J. Gounaris and J. J. Sakurai, Phys. Rev. Lett. **21** (1968) 244.
- [3] J. H. Kühn and A. Santamaria, Z. Phys. **C48** (1990) 445.
- [4] L. M. Barkov et al., Nucl. Phys. **B256** (1985) 365.
- [5] S. Weinberg, Physica **A96** (1979) 327.
- [6] J. Gasser and H. Leutwyler, Ann. Phys. (NY) **158** (1984) 158.
- [7] J. Gasser and H. Leutwyler, Nucl. Phys. **B250** (1985) 465, 517, 539.
- [8] G. Ecker, J. Gasser, H. Leutwyler, A. Pich and E. de Rafael, Phys. Lett. **B223** (1989) 425; G. Ecker, J. Gasser, A. Pich and E. de Rafael, Nucl. Phys. **B321** (1989) 311.
- [9] F. Guerrero and A. Pich, Phys. Lett. **B412** (1997) 382.
- [10] T. N. Truong, Phys. Rev. Lett. **61** (1988) 2526.
- [11] J. Nieves and E. Ruiz Arriola, Nucl. Phys. **A679**, 57 (2000) [hep-ph/9907469].
- [12] T. Hannah, Phys. Rev. **D55** (1997) 5613.
- [13] J. Gasser and Ulf-G. Meißner, Nucl. Phys. **B357** (1991) 90.
- [14] J. Bijnens, G. Colangelo and P. Talavera, JHEP 9805 (1998) 014.
- [15] R. Omnès, Nuovo Cim. **8** (1958) 316; N. I. Muskhelishvili, Singular integral equations (North-Holland, Amsterdam, 1958).
- [16] F. Guerrero, Phys. Rev. **D57** (1998) 4136.
- [17] F. Guerrero and J. A. Oller, Nucl. Phys. B **537**, 459 (1999) [hep-ph/9805334].
- [18] A. Pich and J. Portoles, hep-ph/0101194.
- [19] H. B. O’Connell, B. C. Pearce, A. W. Thomas and A. G. Williams, Prog. Part. Nucl. Phys. **39** (1997) 201.
- [20] F. Guerrero, Estudio del Factor de Forma del Pión, Master Thesis, Univ. Valencia (1996).

- [21] R. Barate et al., Z. Phys. **C76** (1997) 15.
- [22] B. Kubis and Ulf-G. Meißner, Nucl. Phys. **A671** (2000) 331.
- [23] M. Gell-Mann and F. Zachariasen, Phys. Rev. **124** (1961) 953.
- [24] M. Jamin, J.A. Oller and A. Pich, Nucl. Phys. **B587** (2000) 331.
- [25] M. Jamin, J.A. Oller and A. Pich, forthcoming.
- [26] V. Bernard, N. Kaiser and Ulf-G. Meißner, Nucl. Phys. **B364** (1991) 283.
- [27] J. A. Oller and E. Oset, Phys. Rev. **D60** (1999) 074023.
- [28] J. Bijnens, G. Ecker and J. Gasser, Chiral Perturbation Theory in *The DAΦNE Physics Handbook* 2nd edition, editors L. Maiani, G. Pancheri and N. Paver (Frascati).
- [29] J. A. Oller, Phys. Lett. **B477** (2000) 187.
- [30] Ulf-G. Meißner and J. A. Oller, Nucl. Phys. **A673** (2000) 311
- [31] J. A. Oller, E. Oset and A. Ramos, Prog. Part. Nucl. Phys. **45** (2000) 157.
- [32] O. Babelon, J.-L. Basdevant, D. Caillerie and G. Mennessier, Nucl. Phys. **B113** (1976) 445.
- [33] E. G. Floratos, S. Narison and E. de Rafael, Nucl. Phys. **B155** (1979) 115.
- [34] D. Gómez Dumm, A. Pich and J. Portolés, Phys. Rev. D **62** (2000) 054014.
- [35] S. Descotes, hep-ph/0012221.
- [36] S. Descotes and J. Stern, Phys. Lett. **B488**, 274 (2000) [hep-ph/0007082].
- [37] C. Caso et al., The European Physical Journal **C3** (1998) 1.
- [38] S. R. Amendolia et al., Phys. Lett. **B138** (1984) 454; I. B. Vasserman et al., Sov. J. Nucl. Phys. **33** (1981) 709; A. Quenzer et al., Phys. Lett. **B76** (1978) 512; D. Bolini et al., Nuovo Cim. Lett. **14** (1975) 418; G. Barbiellini et al., Nuovo Cim. Lett. **6** (1973) 557; B. Esposito et al., Phys. Lett. **B67** (1977) 239; B. Esposito et al., Nuovo Cim. Lett. **28** (1980) 337.
- [39] G. T. Adylov et al., Phys. Lett. **B51** (1974) 402; Nucl. Phys. **B128** (1977) 461; E. B. Dally et al., Phys. Rev. Lett. **39** (1977) 1176; Phys. Rev. **D24** (1981) 1718.
- [40] P. Estabrooks and A. D. Martin, Nucl. Phys. **B79** (1974) 301.
- [41] B. Hyams et al., Nucl. Phys. **B64** (1973) 134.
- [42] P. M. Ivanov et al., Phys. Lett. **B107** (1981) 297.
- [43] B. Delcourt et al., Phys. Lett. **B99** (1981) 257.
- [44] D. Bisello et al., Z. Phys. **C39** (1988) 13.
- [45] P. M. Ivanov et al., JETP Lett **36** (1982) 112.
- [46] E. B. Dally et al., Phys. Rev. Lett. **45** (1980) 232.
- [47] S. R. Amendolia et al., Phys. Lett. **B178** (1986) 435.
- [48] E. B. Dally et al., Phys. Rev. Lett. **48** (1982) 375.
- [49] W. R. Molzon et al., Phys. Rev. Lett. **41** (1978) 1213.
- [50] NA7 Collaboration, S. R. Amendolia et al., Nucl. Phys. **B277** (1986) 168.
- [51] A. Sirlin, Ann. of Phys. **61** (1970) 294.
- [52] P. Post and K. Schilcher, Phys. Rev. Lett. **79** (1997) 4088.

- [53] J. A. Oller, E. Oset and J. R. Pelaez, Phys. Rev. D **62**, 114017 (2000) [hep-ph/9911297].
- [54] R. Urech, Phys. Lett. **B355**, 308 (1995) [hep-ph/9504238].
- [55] S. Gardner and H. B. O'Connell, Phys. Rev. D **57**, 2716 (1998) [hep-ph/9707385].
- [56] A. G. Williams, H. B. O'Connell and A. W. Thomas, Nucl. Phys. **A629**, 464C (1998) [hep-ph/9707253].